Current injection from a metal to a disordered hopping system. III. Comparison between experiment and Monte Carlo simulation

S. Barth, U. Wolf, and H. Bässler
Institute of Physical, Nuclear and Macromolecular Chemistry and Center of Material Science, Philipps-University of Marburg, Hans-Meerwein-Straße, D-35032 Marburg, Germany

P. Müller, H. Riel, H. Vestweber, P. F. Seidler, and W. Rieß
IBM Research, Zurich Research Laboratory, CH-8803 Rüschlikon, Switzerland
(Received 12 April 1999)

We have performed electric-field and temperature-dependent electron injection studies in an aluminum/tris(8-hydroxy-quinolinolato)aluminum/magnesium:silver single-layer organic light-emitting diode. Analysis of the observed injection currents in terms of the classic Fowler-Nordheim (FN) tunneling or Richardson-Schottky (RS) thermionic emission proved to be inadequate. Whereas, the FN-type behavior at high-electric fields must be considered accidental, the injection currents qualitatively resemble those of the RS concept. However, quantitative differences are observed concerning the RS coefficient, the prefactor current, and the temperature dependence. On the other hand, the experimental data are in excellent agreement with a recently presented Monte Carlo simulation [U. Wolf *et al.*, Phys. Rev. B **59**, 7507 (1999)] of carrier injection from a metal to an organic dielectric with random hopping sites. [S0163-1829(99)14535-1]

I. INTRODUCTION

In recent years, organic light-emitting diodes (OLED's) have been comprehensively studied for their possible application in displays.[1–9] To improve their efficiency, a detailed understanding of the charge-carrier injection processes is necessary. Charge-carrier injection from a metallic contact into solids, and especially into semiconductors, has been extensively investigated,[10] and it is well known that the energy barrier between the contact and the organic dielectric controls the hole and electron injection. In the absence of surface states and a depletion region due to impurity doping,[11] the energy barrier is $\Delta_h = I - \Phi_{\text{anode}}$ for holes and $\Delta_e = \Phi_{\text{cathode}} - A$ for electrons,[12] where Φ is the work function of the contact material and I and A are the ionization energy and electron affinity of the organic dielectric, respectively. Depending on the magnitude of Δ, the current flowing through an OLED can either be space-charge limited (SCL), i.e., transport limited, or injection limited. A necessary condition for SCL conduction is that one of the contacts supply more charge carriers per unit time than can be transported through the organic dielectric.[12–16] A contact that behaves in this way is called an ohmic contact. At an ohmic contact the electric field F vanishes owing to screening by the space charge associated with unipolar current flow. This requires an injection barrier small enough to guarantee efficient injection without the assistance of an external electric field. The SCL current (SCLC) is the maximum unipolar current a sample can sustain at a given electric field unless the exit contact is able to inject opposite charge carriers sufficient to compensate for the internal space charge. In the absence of traps the SCLC obeys Child's law

$$j_{\text{SCL}}(F) = \frac{9}{8}\varepsilon\varepsilon_0\mu\frac{F^2}{L}, \tag{1}$$

where ε is the relative dielectric constant, ε_0 the permittivity of vacuum, μ the charge-carrier mobility, and L the sample thickness.

Injection-limited conduction is commonly described either by the Fowler-Nordheim (FN) model for tunneling injection or by the Richardson-Schottky (RS) model for thermionic emission.[17] The FN model ignores image-charge effects and considers the tunneling of electrons from the contact through a triangular barrier into unbound continuum states. It predicts a $j(F)$ characteristic, which is insensitive to temperature,

$$j_{\text{FN}} = BF^2 \exp\left[-\frac{b}{F}\right], \tag{2}$$

where $B = e^3/8\pi h\Delta$ and $b = [8\pi(2m^*)^{1/2}\Delta^{3/2}]/3he$. Here e is the elementary charge, h the Planck constant, and m^* the effective mass of the carrier inside the dielectric.

The RS model assumes that an electron from the contact can be injected once it has acquired a thermal energy sufficient to cross the potential maximum resulting from the superposition of the external and the image-charge potential. Tunneling through the barrier is ignored. The $j(F)$ characteristic is given by

$$j_{\text{RS}} = A^*T^2 \exp\left[-\frac{\Delta - (e^3/4\pi\varepsilon\varepsilon_0)^{1/2}F^{1/2}}{kT}\right], \tag{3}$$

where A^* is the Richardson constant, T the temperature, and k the Boltzmann constant.

The models described above were developed for bandtype materials, and it is difficult to rationalize an application of these models to disordered organic materials, where the charge-carrier mobility is low (typically $\mu \ll 10^{-3}$ cm^2/Vs), which means that charge carriers are localized and transport involves discrete hopping within a distribution of energy

states. Recently, various Monte Carlo simulation studies[18,19] and analytic theories[20,21] were presented for the charge-carrier injection into an organic hopping system. Gartstein and Conwell[19] investigated how charge carriers generated within a Gaussian density of states under the premise of either unrelaxed or relaxed starting energy escape from a Coulombic potential. Arkhipov *et al.*[20] presented an analytic theory that explicitly includes the primary injection step from the Fermi level of the metal to the first layer of the dielectric, whereas the subsequent diffusive random walk is treated in terms of an Onsager-like process. Wolf *et al.*[18] recently performed more detailed Monte Carlo simulations under the premise that thermal injection starts from the Fermi level of an electrode and populates states under the manifold of hopping states according to a weighted probability density that takes into account thermal activation and the energetic distribution of hopping states. Arkhipov *et al.*[21] compared these simulations with the results of an analytic theory and found good agreement for the field dependence of the yield of charge carriers as a function of the energy barrier at the metal/organic-dielectric interface.

The aim of the present paper is to analyze electron-injection studies performed with a single-layer OLED consisting of aluminum/tris(8-hydroxy-quinolinolato) aluminum (Alq_3)/magnesium:silver alloy in terms of the classical FN tunneling and RS thermionic emission models. Alq_3, the most common electron-transporting and emitting material in OLED's, was used for these investigations because of its nearly pinhole-free, film forming characteristics, good charge-carrier transport properties, and high-thermal stability. Furthermore, detailed investigations of single-layer Alq_3 devices with different anode and cathode materials showed that Al/Alq_3/Mg:Ag structures are electron-only devices and thus are an ideal system to study electron injection and transport.[22]

The experimental results will be compared to recent Monte Carlo simulations by Wolf *et al.*[18]

II. EXPERIMENT

Our OLED's consist of glass substrates (7059 Corning) covered with an evaporated Al anode, followed by a 150 nm-thick Alq_3 layer as active material and a Mg:Ag (10:1) alloy as metal top cathode. The schematic device structure together with the energy-level diagram and the molecular structure of Alq_3 are shown in Fig. 1.

All layers were prepared in a high-vacuum system (Leybold) by vapor deposition using resistively heated tantalum and tungsten boats. The typical deposition rate for Alq_3 and the metals/alloys was about 1 Å/s. For the deposition of the Mg:Ag alloy the evaporation rates of Mg and Ag were controlled independently by separate thin-film deposition monitors (Leybold Infikon). The active area of our devices was 2×2 mm^2, and the base pressure in the chamber ranged between 10^{-7} and 10^{-6} mbar. The evaporation chamber was attached directly to a glovebox, allowing device fabrication and characterizations completely under inert (argon) conditions.

The current-voltage (I-V) characteristics were measured with a Hewlett Packard Parameter Analyzer (HP 4145 B). Our temperature-dependent measurements of the I-V characteristics were performed in a specially designed setup, which allows temperatures as low as 77 K (liquid nitrogen). The temperature of the sample was measured via two thermocouples (NiCr/NiAl, Thermocoax) placed directly above and below the device. To ensure reproducibility of the data the measurements of the I-V curves were performed in a temperature cycle, i.e., the data were taken in both temperature sweep directions. Constant temperature conditions were obtained with extremely long temperature-stabilizing times.

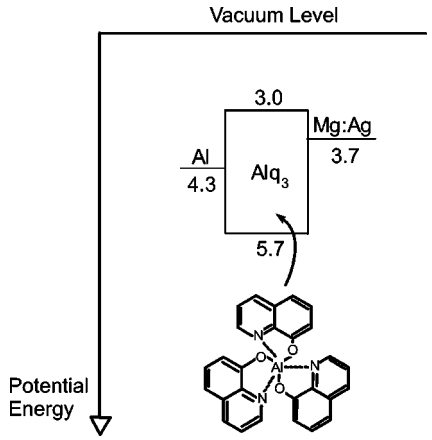

FIG. 1. Schematic energy-level diagram, device structure, and molecular structure of Alq_3.

The charge-carrier injection from a metal contact into a random organic dielectric has been studied via Monte Carlo simulations. A detailed description of the simulation technique can be found in Ref. 18.

III. RESULTS

Figure 2 presents a series of I-V characteristics parametric in the temperature for an Al/Alq_3(150 nm)/Mg:Ag device. The I-V curves were measured subsequently, starting at higher temperatures. They show a typical diode behavior featuring a steep increase in current in forward direction, indicating efficient charge-carrier injection and transport above a certain voltage. With decreasing temperature the threshold voltage shifts to higher voltages. The detection limit of the current is determined by the setup and the occurrence of leakage currents. It is noteworthy that the currents at 133 K differ from those at room temperature by more than three orders of magnitude at the same voltage. Figure 3 shows I-V curves measured in a temperature cycle. These data clearly manifest that absolute currents are reproducible within a factor of 2, and do not exhibit a pronounced hysteresis effect.

IV. DISCUSSION

The interpretation of the present electron-injection studies performed with an Al/Alq_3(150 nm)/Mg:Ag device in terms of Child's law of SCLC will fail. Although the I-V characteristics shown in Fig. 2 bear out a power-law behavior of $I\propto V^7$ for 295 K and $I\propto V^{12}$ for 133 K, indicative of trap-controlled SCLC flow, this has to be considered accidental because of the absence of an ohmic contact in our device. In view of the present energy barrier for electron injection, it is all but surprising that the currents are injection rather than space-charge limited.

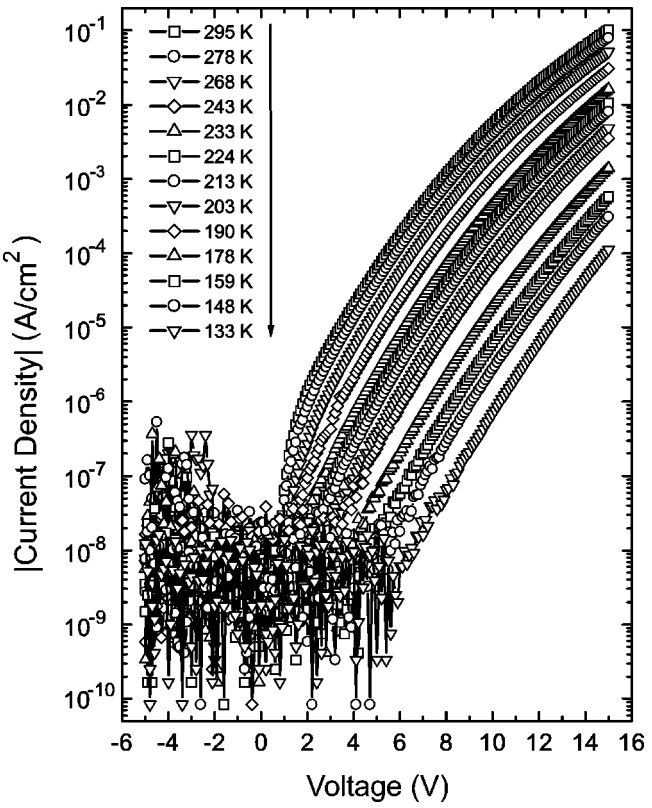

FIG. 2. *I-V* characteristics of an Al/Alq_3(150 nm)/Mg:Ag device at various temperatures. Data were taken in a temperature scan from 295 to 133 K.

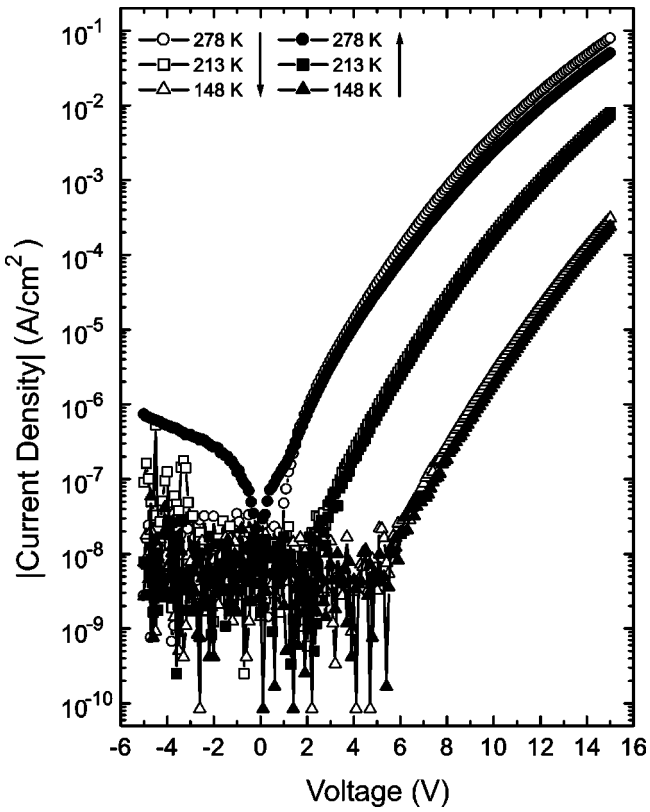

FIG. 3. *I-V* characteristics of an Al/Alq_3(150 nm)/Mg:Ag device. Data represented by open and solid symbols were taken in a temperature cycle, i.e., at falling and rising temperatures, respectively. The *I-V* curves indicate both the absence of pronounced hysteresis effects and the level of reproducibility of absolute currents.

Therefore, we will analyze the *I-V* characteristics (Fig. 2) in terms of injection-limited currents. Often, injection-limited currents in OLED's dominated by majority carriers at high-electric fields have been treated in terms of the classic FN model for tunneling injection. The FN plots, $\ln(j_{FN}/F^2)$ vs F^{-1}, often feature an asymptotic straight-line behavior, and from the slope of these lines one arrives at values for the injection barrier.[23–25] In the literature, e.g., Refs. 23–25, the energy barrier correlates reasonably well with barriers expected on the basis of the highest occupied molecular orbital/lowest unoccupied molecular orbital (LUMO) of the active material and the idealized work functions of the electrodes. Figure 4 shows the experimental data of Fig. 2 in an FN plot. For this representation a built-in voltage of 0.7 eV from the difference in the work functions of Al and Mg:Ag alloy was taken into consideration. In the high-field range the curves were fitted linearly, and because we have an electron-only device, one can calculate from the slope the values of the barrier height for electron injection from the Mg:Ag cathode into the Alq_3 layer. The energy barriers obtained vary between 0.18 and 0.3 eV at 295 and 133 K, respectively. However, these barriers are significantly lower than expected on the basis of the LUMO of Alq_3 and the Fermi level of the Mg:Ag cathode obtained from the energy-level diagram (Fig. 1) and imply that our experimental results cannot be described by the FN tunneling model and that the FN-type $j(F)$ characteristics at high-electric fields have to be considered accidental. Further arguments against the appropriateness of the FN theory are the strong temperature dependence of the currents observed even at higher electric fields and the saturation of the currents at lower fields ($<2\times10^5$ V/cm). Therefore, we conclude that tunneling is not involved. This conclusion is supported by a recent Monte Carlo simulation[18] and an analytic theory.[21] In the former, the unimportance of long-range tunneling transitions is demonstrated for various jumping distances between the metal and the adjacent layer of the amorphous organic dielectric. In the latter the rate-limiting step is the primary injection event from the metal into the dielectric, which has been treated in terms of hopping theory involving the concept of transport energy. The agreement of the field dependences of the injection current from simulation studies and from analytic theory in this paper is remarkable.[21]

The above brief analysis clearly demonstrates that the FN tunneling concept is obviously not appropriate to describe the electron injection in our single-layer OLED. Therefore, we try to analyze the experimental results in terms of the RS concept of thermionic emission. Equation (3) predicts that a $\ln j_{RS}$ vs $F^{1/2}$ plot parametric in temperature should feature a family of straight lines. In Fig. 5, the *I-V* characteristics of Fig. 2 are plotted in a $\log_{10} j_{RS}$ vs $F^{1/2}$ representation, at which the built-in potential of 0.7 eV was subtracted from the voltage applied to the device. For the entire temperature range investigated one observes a linear relationship between current density and $F^{1/2}$ in the semilogarithmic plot except for current densities $\leqslant 10^{-8}$ A/cm^2 because of the low signal-to-noise ratio caused by limitations of the experimen-

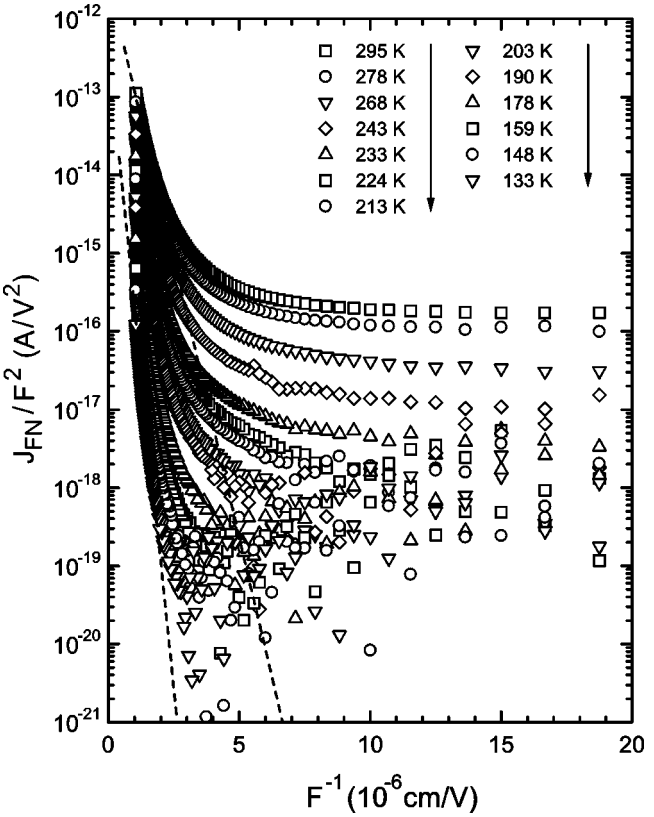

FIG. 4. Fowler-Nordheim representation of the data shown in Fig. 2. A built-in voltage of 0.7 eV was taken into consideration. From the slope of the dashed lines the energy barrier for the electron injection at the Mg:Ag| Alq_3 interface was calculated. The energy barrier ranges from 0.18 to 0.3 eV for 295 and 133 K, respectively.

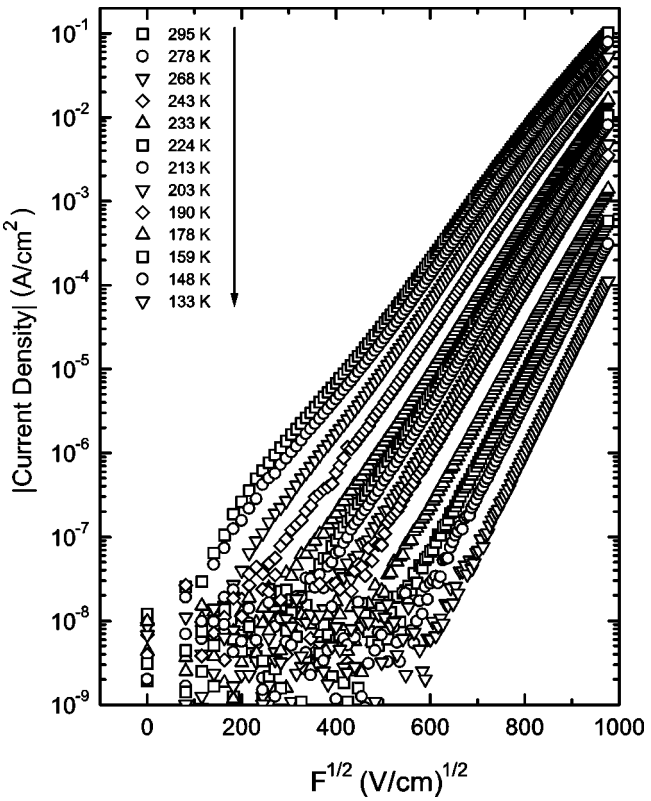

FIG. 5. Representation of the *I-V* characteristics shown in Fig. 2: |current density| vs $F^{1/2}$ on a $\log_{10}$ scale (Richardson-Schottky plot). A built-in voltage of 0.7 eV was taken into consideration.

tal setup. In the following we will show that the experimental data resembles the predictions of RS theory, but that differences exist concerning the quantitative data analysis. By extrapolating the straight lines in Fig. 5 to $F=0$, the current densities at zero electric field (J_0) were determined as a function of temperature. Presuming the validity of the RS concept one can calculate the energy barrier for the injection of electrons from the Mg:Ag electrode into Alq_3 to be 0.32 eV [Fig. 6(a)]. This concept assumes that injection occurs into unbound electron states obeying a parabolic energy-versus-momentum dependence, $F(k)$, where k is the momentum vector in the direction of the electron surface.[17] The T^2 term in the RS Eq. (3) results from integration over k space. However, in a disordered hopping system no unbound electron states exist, and injection events occur via the first layer of the dielectric in the course of an optimization procedure concerning site energy and density of states (DOS). Therefore, it is illegitimate to integrate over k space for an organic dielectric. This allows one to abandon the T^2 factor in the RS equation for the calculation of the energy barrier. In Fig. 6(b) the current densities J_0 are shown in a $\log_{10} J_0$ vs $1/T$ plot in which the T^2 term has been neglected. An energy barrier of 0.5 eV is obtained from the high-temperature asymptote. Besides, the prefactor current of the injection rate into a two-dimensional sheet of hopping sites should differ from the one predicted by the RS theory. Extrapolating J_0 to $T\rightarrow\infty$ would yield a value of $A^*\cong 1.5\times 10^{-8}$ A/cm^2 K^2, whereby the theoretical value is 120 A/cm^2 K^2 (Ref. 17).

Another discrepancy from the thermionic emission concept is found concerning the temperature dependence of the injection current at different electric fields [Fig. 6(c)]. The current density approaches an Arrhenius law at high temperatures but levels off gradually at lower temperatures. Previous Monte Carlo simulations of geminate pair dissociation[26] and experiments on both intrinsic and extrinsic photoconduction[27] also show that such a sublinear temperature dependence is a ubiquitous feature of energetically random hopping systems. The reason is that within a Gaussian distribution of energy states, charge carriers tend to relax energetically towards lower localized states.[28,29] Under stationary conditions an ensemble of carriers shift by an energy of $\varepsilon_\infty=-\sigma^2/kT$ relative to the center of the DOS, where σ is the variance of the DOS. However, the actual injection process occurs far away from equilibrium. By lowering the temperature and increasing the width of the Gaussian DOS the ensemble of injected charge carriers will move further away from equilibrium. Therefore, the injection process becomes more efficient as the system deviates from equilibrium. At higher temperatures the disorder effect vanishes and the rate-limiting step approaches that determined by the Boltzmann factor taking field-induced barrier lowering into account, i.e., $\exp\{-[\Delta-(\varepsilon^3F/4\pi\varepsilon\varepsilon_0)^{1/2}]/kT\}$. This is illustrated in terms of the high-temperature asymptotes shown in Fig. 6(c), which result in energy barriers of 0.16, 0.21, 0.25, and 0.30 eV at electric fields of 9.5×10^5, 7×10^5, 5×10^5, and 3×10^5 V/cm, respectively. The basic result is that energy barriers calculated from a $\ln j$ vs $1/T$ plot, especially near ambient temperature and at high-electric fields, will un-

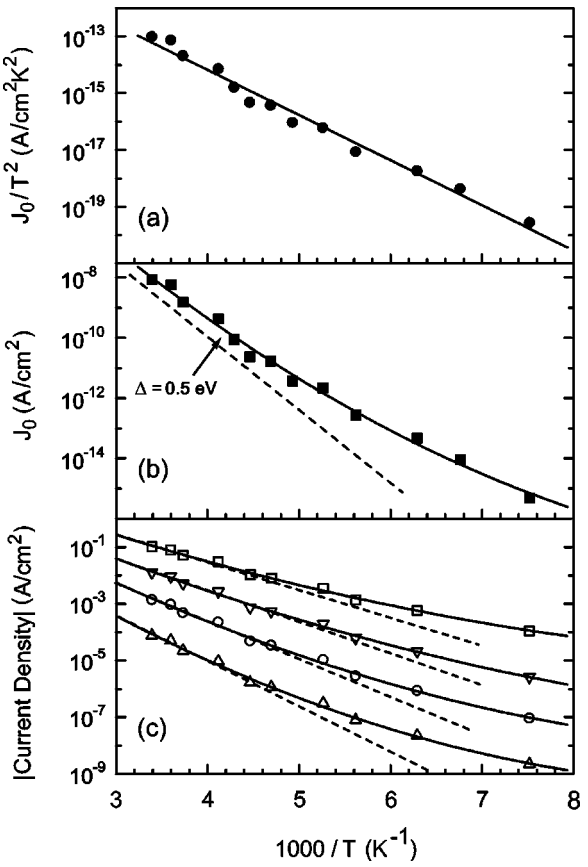

FIG. 6. (a) Relationship between J_0/T^2 and $1/T$. The current densities at zero-electric field (J_0) were obtained by extrapolating the lines in Fig. 5 to the ordinate. From the slope of the solid line the energy barrier for electron injection at the Mg:Ag| Alq_3 interface is determined to be 0.32 eV, and from the ordinate intercept the Richardson constant is calculated to be $A^*=1.5\times10^{-8}$ A/cm^2 K^2. (b) Relationship between J_0 and $1/T$. From the high-temperature asymptote an energy barrier of 0.5 eV is obtained for electron injection from the Mg:Ag cathode to the Alq_3 layer. (c) Temperature dependence of the current density for different electric fields for an Al/Alq_3(150 nm)/Mg:Ag device. The high-temperature asymptotes result in energy barriers of 0.16, 0.21, 0.25, and 0.30 eV at electric fields of 9.5×10^5 (□), 7×10^5 (▽), 5×10^5 (○), and 3×10^5 (△) V/cm, respectively.

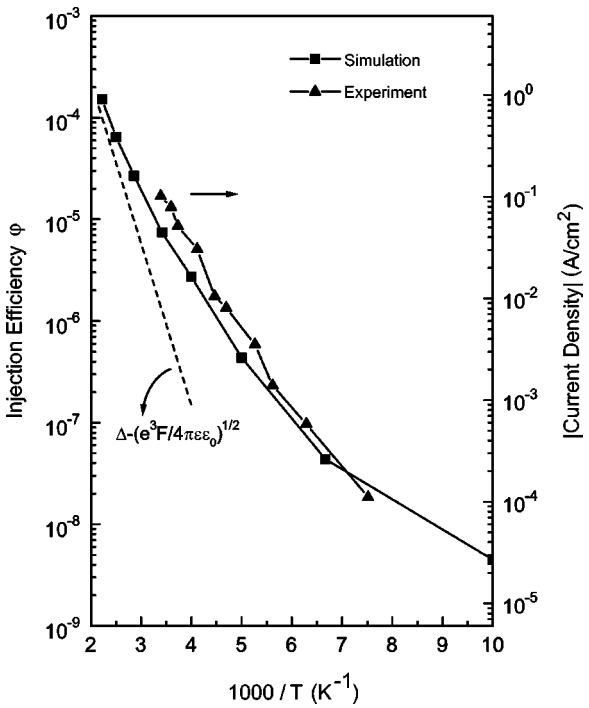

FIG. 7. Comparison of the temperature dependence of the injection efficiency (φ) between a disordered hopping system characterized by a Gaussian DOS (variance $\sigma=100$ meV, zero-field energy barrier $\Delta=0.5$ eV, electric field $F=1\times10^6$ V/cm) and experimental data of the current density obtained from an Al/Alq_3(150 nm)/Mg:Ag device at 9.5×10^5 V/cm. The dashed line represents the high-temperature asymptote for an energy barrier of $\Delta-(e^3F/4\pi\varepsilon\varepsilon_0)^{1/2}$ eV.

derestimate the real energy barrier height. This conclusion is based on the comparison between the temperature dependence of the injection efficiency (φ) in a disordered model hopping system determined via computer simulation, and experimental data for the injection current obtained at $F=9.5\times10^5$ V/cm (Fig. 7). Assuming a zero field-injection barrier of $\Delta=0.5$ eV and a variance of $\varphi=100$ meV for the manifold of hopping states, the temperature dependence of the injection current measured at an electric field of 1×10^6 V/cm can be modeled over more than three orders of magnitude with remarkable accuracy. This demonstrates that the concept of temperature and field-assisted injection into a random hopping system can quantitatively describe the experimental observations. We emphasize that this concept involves Miller-Abrahams-type jump rates rather than polaron rates.[30] This result is consistent with analyses of the temperature and field dependence of the charge-carrier mobility in a broad class of organic glasses known to feature a Gaussian DOS about 100-meV wide.[31,32] Another conclusion from the comparison of theory and experiment is that a simple Arrhenius analysis of the temperature dependence of the current, notably at a restricted temperature range and a high-electric field, would widely underestimate the true zero-field barrier. For example, if one calculates the slope of the ln j vs $1/T$ plot near 300 K, one would arrive at a value of $\cong0.2$ eV. Considering the barrier lowering of 0.2 eV at $F=1\times10^6$ V/cm, the asymptotic value at this field is $\cong0.3$ eV.

Simulation also provides an estimate of the injection current from a Mg:Ag contact into Alq_3 in the $T\rightarrow\infty$ and/or $F\rightarrow\infty$ limit. Yielding the probability for a carrier once attempting to cross the barrier, it is to estimate how many electrons are available per attempt at a given temperature and field. As at $T=295$ K and $F=9.5\times10^5$ V/cm, we have $j\cong10^{-1}$ A/cm^2, we obtain a limiting current density of 10^4 A/cm^2 for $\varphi\cong10^{-5}$. Recalling that RS theory would predict $j_\infty\cong6\times10^6$ A/cm^2, one has to consider, however, that the attainment of such large current densities requires extremely thin samples and/or large carrier mobilities to avoid field screening at the electrode due to space-charge accumulation. On the other hand this estimate suggests that under appropriate experimental conditions the current densities required to achieve electrically driven lasing in OLED's might be feasible.

Finally we comment on another difference between the classic RS model and thermally assisted hopping injection. For an organic layer with a dielectric constant of $\varepsilon=3.5$ the RS coefficient should be $\beta_{RS}=(e^3/4\pi\varepsilon\varepsilon_0)^{1/2}/kt=0.77$

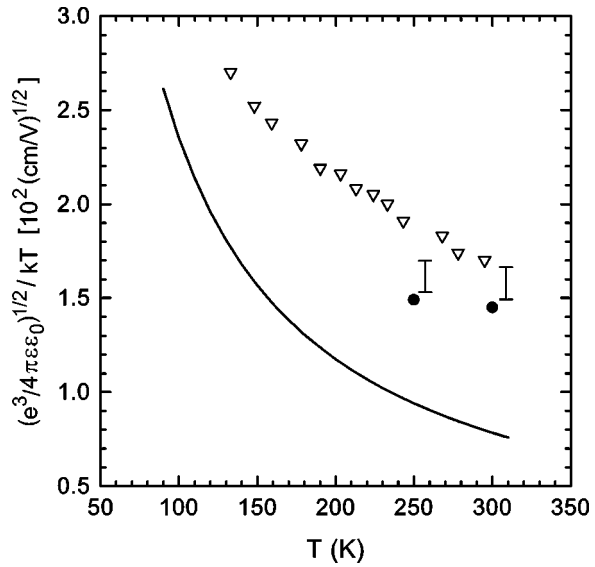

FIG. 8. Comparison of the theoretical Richardson-Schottky coefficient $\beta_{RS}=(e^3/4\pi\varepsilon\varepsilon_0)^{1/2}/kt$ for $\varepsilon=3.5$ (solid line), the experimental data for Alq_3 ($\triangledown$) obtained from the slopes of the straight lines in Fig. 5, and the simulation values at 250 and 300 K ($\bullet$) for a disordered hopping system characterized by a Gaussian DOS with $\sigma=80$ meV.

$\times 10^{-2}$ (cm/V)$^{1/2}$ at 300 K. For a Gaussian distribution of hopping states of variance $\sigma=80$ meV simulation predicts β_{RS} to be $1.4\ldots1.5\times10^{-2}$ (cm/V)$^{1/2}$. From the slopes of the straight lines in Fig. 5 the experimental β_{RS} values for Alq_3 can be calculated. These data are plotted in Fig. 8 as a function of the temperature together with the theoretical curve and values for a disordered hopping system. Although the *I-V* characteristics follow qualitatively the prediction of the RS concept (Fig. 5), there obviously exist quantitative differences as far as the RS coefficient is concerned. The theoretical β_{RS} values are a factor of $\cong 2$ lower than the experimental data.

V. CONCLUSIONS

In the present paper we have investigated the electron injection in an Al/Alq_3(150 nm)/Mg:Ag single-layer OLED. Conventional models such as Fowler-Nordheim tunneling and Richardson-Schottky thermionic emission cannot account for the experimentally observed dependence of the injection current on electric field and temperature. The similarity with FN-type $j(F)$ characteristics at high-electric fields has to be considered accidental. Analysis of the injection current in terms of the classic RS concept yields only qualitative agreement with the experimental data. Quantitative differences are noted concerning the RS coefficient (β_{RS}), the RS constant (A^*), and the temperature dependence. We find excellent agreement with experiment, provided by a Monte Carlo simulation,[18] which takes into account that thermal injection starts at the Fermi level of an electrode and populates states under the manifold of hopping states according to a weighted probability density of width 100 meV, assuming a zero-field energy barrier of $\Delta=0.5$ eV. Given the uncertainty of the exact values of the work functions of Mg:Ag and the reduction potential of Alq_3, this agreement is quite satisfactory.

ACKNOWLEDGMENTS

This work was supported by the Deutsche Forschungsgemeinschaft (SFB 383). S. Barth thanks the IBM Zurich Research Laboratory for hosting his visit.

[1] C. W. Tang and S. A. Van Slyke, Appl. Phys. Lett. **51**, 913 (1987).
[2] C. W. Tang, S. A. Van Slyke, and C. H. Chen, J. Appl. Phys. **65**, 3610 (1989).
[3] C. Adachi, T. Tsutsui, and S. Saito, Appl. Phys. Lett. **56**, 799 (1990).
[4] J. Kido, M. Kimura, and K. Nagai, Science **267**, 1322 (1995).
[5] T. Wakimoto, R. Murayama, K. Nagayama, Y. Okuda, H. Nakada, and T. Tohma, in *Proceedings SID'96 International Symposium, Digest of Technical Papers, San Diego, CA, 1996*, edited by J. Morreale (Society for Information Display, Santa Ana, 1996), Vol. XXVII, p. 849.
[6] H. Nakada and T. Tohma, in *Proceedings of the International Symposium on Inorganic and Organic Electroluminescence*, edited by R. H. Mauch and H.-E. Gumlich (Wissenschaft und Technik Verlag, Berlin, 1996), p. 385.
[7] H. Nakamura, C. Hosokawa, and T. Kusumoto, in *Proceedings of the International Symposium on Inorganic and Organic Electroluminescence* (Ref. 6), p. 95.
[8] Y. Hamada, T. Sano, H. Fujii, Y. Nishio, H. Takahashi, and K. Skibata, Jpn. J. Appl. Phys., Part 1 **35**, 1339 (1996).
[9] For recent progress, see *Organic Electroluminescent Materials and Devices*, edited by S. Miyata and H. S. Nalwa (Gordon and Breach, Lausanne, 1997).
[10] E. H. Rhoderick and R. H. Williams, *Metal-Semiconductor Contacts* (Clarendon Press, Oxford, 1988).
[11] M. Meier, S. Karg, and W. Rieß , J. Appl. Phys. **82**, 1961 (1997).
[12] M. Pope and C. E. Swenberg, *Electronic Processes in Organic Crystals* (Clarendon Press, Oxford, 1982).
[13] W. Helfrich, in *Physics and Chemistry of the Organic Solid State*, edited by D. Fox, M. M. Labes, and E. Weissberger (Wiley, New York, 1967), Vol. III, p. 1.
[14] M. A. Abkowitz and D. Pai, Philos. Mag. B **53**, 193 (1986).
[15] P. W. M. Blom, M. J. M. de Jong, and J. J. M. Vleggaar, Appl. Phys. Lett. **68**, 3308 (1996).
[16] A. J. Campbell, D. D. C. Bradley, and D. G. Lidzey, J. Appl. Phys. **82**, 6326 (1997).
[17] Ch. Weißmantel and C. Hamann, *Grundlagen der Festkörperphysik* (VEB Deutscher Verlag der Wissenschaften, Berlin, 1981).
[18] U. Wolf, V. I. Arkhipov, and H. Bässler, Phys. Rev. B **59**, 7507 (1999).
[19] Yu. N. Gartstein and E. M. Conwell, Chem. Phys. Lett. **255**, 93 (1996).
[20] V. I. Arkhipov, E. V. Emelianova, Y. H. Tak, and H. Bässler, J. Appl. Phys. **84**, 848 (1998).
[21] V. I. Arkhipov, U. Wolf, and H. Bässler, Phys. Rev. B **59**, 7514 (1999).

[22] H. Riel, Diploma thesis, University of Erlangen-Nürnberg, Germany, 1998.
[23] I. D. Parker, J. Appl. Phys. **75**, 1656 (1994).
[24] A. I. Heeger, I. D. Parker, and Y. Yang, Synth. Met. **67**, 23 (1994).
[25] H. Vestweber, J. Pommerehne, R. Sander, R. F. Mahrt, A. Greiner, W. Heitz, and H. Bässler, Synth. Met. **68**, 263 (1995).
[26] U. Albrecht and H. Bässler, Chem. Phys. Lett. **199**, 297 (1995).
[27] S. Barth, D. Hertel, Y. H. Tak, H. Bässler, and H.-H. Hörhold, Chem. Phys. Lett. **274**, 165 (1997).
[28] B. Ries, H. Bässler, M. Grünwald, and B. Movaghar, Phys. Rev. B **37**, 5508 (1988).
[29] B. Movaghar, B. Ries, and M. Grünwald, Phys. Rev. B **34**, 5574 (1986).
[30] M. N. Bussac, D. Michoud, and L. Zuppiroli, Phys. Rev. Lett. **81**, 1678 (1998).
[31] H. Bässler, Phys. Status Solidi B **175**, 15 (1993).
[32] D. H. Dunlap, P. E. Parris, and V. M. Kenkre, Phys. Rev. Lett. **77**, 542 (1996).